

Tuned Pd/SiO₂ aerogel catalyst prepared by different synthesis techniques

L.M. Sanz-Moral¹, A. Romero¹, F.Holz², M. Rueda¹, A.Navarrete¹, A. Martín^{1*}.

¹High Pressure Processes Group, Department of Chemical Engineering and Environmental Technology, University of Valladolid, Doctor Mergelina s/n,47011 Valladolid, Spain

²Ruhr Universität Bochum, Universitätsstr. 150, 44801 Bochum, Germany

Tel: +34 983184077 e-mail: mamaan@iq.uva.es (Á. Martín)

Tuned Pd/SiO₂ aerogel catalyst prepared by different synthesis techniques

L.M. Sanz-Moral¹, A. Romero¹, F.Holz², M. Rueda¹, A.Navarrete¹, A. Martín^{1*}.

¹High Pressure Processes Group, Department of Chemical Engineering and Environmental Technology, University of Valladolid, Doctor Mergelina s/n,47011 Valladolid, Spain

²Ruhr Universität Bochum, Universitätsstr. 150, 44801 Bochum, Germany

Tel: +34 983184077 e-mail: mamaan@iq.uva.es (Á. Martín)

Abstract

Pd nanoparticles have been embedded on silica aerogel by using three different techniques. In each of them the metal was loaded in the matrix at different steps of the production: the direct synthesis, the wet impregnation and the supercritical impregnation of the previously dried aerogels. The resultant materials have been characterized to analyze the differences depending on the applied technique for its impregnation. Atomic absorption, nitrogen physisorption, X-ray diffraction, infrared spectroscopy and transmission electron microscopy were performed. In all the techniques the concentration of metal has been varied (from 0.13 to 1.61 % wt.) by modifying the concentration of the suspension (Pd-polyvinylpyrrolidone nanoparticles used in the direct synthesis) or of the solution of the metallic precursor (palladium acetylacetonate), both in the organic solvent and the supercritical media. The characterization had generally shown a good distribution of the metallic particles in the matrix, and the negligible effect of the metal on the textural properties. Finally, considerable variations were observed on the silanol groups on the surface of the catalysts. These materials were tested in D-glucose hydrogenation, observing significant

differences on the performance of the catalyst depending on the synthesis technique employed.

Keywords aerogel; silanol; tuned selectivity; palladium catalyst; nanoparticles; supercritical CO₂

1. INTRODUCTION

Effective routes to obtain more valuable products require the design of efficient catalysts. Novel catalytic structures are therefore needed to overcome the present challenges. These novel structures require the integration of support active sites in a way that preserves their advantages and capabilities. Therefore the development of novel catalytic structures achieved by the integration of metallic nanoparticles evenly distributed in a mesoporous and high-surface aerogel appears as a promising alternative. Silica aerogels present remarkable properties which make them suitable materials to overcome these new challenges: high pore volumes, favorable transport properties, stability and surface activity. What is more, their properties can be easily tuned: their textural properties can be tailored by changing the ratios of precursor [1]; the chemistry of their surface can be controlled by using different alkyl-alkoxy/chloro silanes allowing to govern their grade of hydrophobicity [2]; in addition, the option of creating hybrid aerogels make almost all properties requirements achievable [3].

By contrast, due to its breakability special techniques must be applied for the metal impregnation before or after the drying in order to avoid the capillarity forces which could damage the structure of the matrix. Cogelled aerogel and Impregnated Aerogel Catalysts were already produced [4], concluding that the cogelled ones showed better resistance to sintering. Also Ni and Pd nanoparticles were embedded on aerogels by impregnation of the gels followed by supercritical drying [5]. Ionic liquids have also been considered as a possible route [6]. Finally supercritical CO₂ has been used as

impregnation media and 1,1,1,5,5,5-Hexafluoro-2,4-pentanedione-palladium (2:1) as metal precursor [7]. Furthermore, the solubility of Palladium(II) acetylacetonate in supercritical CO₂ has been already studied, providing another Pd precursor which could be used in the supercritical impregnation (SCI) technique[8].

Therefore, different preparation techniques have been proposed for incorporating Pd catalytic nanoparticles in a silica matrix, showing different results depending on the technique employed. But to our knowledge, a systematic study of the variation of the final properties of the materials depending on the techniques and solvents used for the metal impregnation has not been done. What is more, this variation of properties could be translated into differences on the functionality of the final catalysts.

Catalytic hydrogenation of D-glucose into sorbitol seems to be a simple reaction, but in fact D-glucose can follow different reaction pathways instead of being converted into sorbitol. In essence, D-glucose can isomerize into D-fructose by Lobry de Bruyn Alberda – Van Ekenstein reaction [9] and its subsequent hydrogenation allows to obtain mannitol / sorbitol mixture[10]. In addition, byproducts such as glycolaldehyde and glyceraldehyde could appear as a result of retro aldol condensation reaction [11], which are hydrogenated into smaller sugar alcohols like ethylene glycol and glycerol respectively. Ru-based catalysts demonstrated to be the most effective for catalytic hydrogenation into sorbitol. However, metals such as Ni, Pt, Pd and Rh have been used for similar purposes due to their lower price in comparison with Ru [12]. Bizhanov et al. reported that the combination of Pd and Ni in the hydrogenation of D-glucose was very effective in comparison with other bimetallic catalysts [13].

In this work, Pd nanoparticles have been embedded on silica aerogel by using three different techniques. In each of them the metal was loaded in the matrix at different steps of the production: the direct synthesis (DS), the wet impregnation (WI), and the

SCI of the previously dried aerogels. Kinetic tests of D-glucose hydrogenation into sugar alcohols were carried out in order to check the catalytic behavior of the catalysts. The influence of the preparation technique in the activity of each catalyst was reported.

2. EXPERIMENTAL

2.1 Reagents

Tetramethoxysilane (TMOS, 98%), Palladium(II) acetylacetonate (Pd(acac)₂, 99%), Polyvinylpyrrolidone (PVP) average mol wt 10,000, Borane-ammonia complex (97%) and D-(+)-glucose (≥99.5%) were purchased from Sigma–Aldrich. Methanol (99.8%) and ammonium hydroxide (25%) were obtained from Panreac. CO₂ (>99.95 mol%) and technical H₂ were supplied by Carbueros Metálicos S.A. Deionized water was used in all experiments.

2.2 Aerogels synthesis:

Hydrophilic silica alcogels were produced following the single step sol–gel process [14]. The molar ratio was TMOS:CH₃OH:H₂O:NH₄OH, 1:2.3:3.8:1.2 × 10⁻². Then the alcogels were dried by using supercritical CO₂. The drying took place in a closed circuit where the CO₂ at 10.5 MPa and 45°C was recirculated till the solvent was completely removed. Three loads of fresh CO₂ where needed. A detailed description of the setup can be found elsewhere [15].

2.2.1 Palladium impregnation

Three different techniques were used to impregnate Pd into the silica matrix by using the same metal precursor.

The first one was the traditional WI method, which consisted on adding Pd(acac)₂ into the aging solvent. That was followed by the supercritical drying with CO₂. Two solvents were used: methanol and acetone. Acetone one was chosen because of the higher solubility of the precursor. The solutions were saturated at 20, 40 and 50°C.

The second one was the SCI. It is based on the dissolution-precipitation principle. After the supercritical drying of aerogels, the supercritical CO₂ was also used as solvent media for the Pd(acac)₂. The precursor was placed in excess in a batch reactor where the samples stayed at 25 MPa and 60°C for a long time to secure the solubilization till saturation conditions and diffusion of the metal precursor. Then the solubility of the precursor was decreased to force its precipitation into the aerogels pores by reducing temperature till room temperature. Finally the system was decompressed at a rate of 0.3 MPa/min.

The third one, the DS, was made by suspending metallic Pd nanoparticles in the methanol of the alcogels synthesis. These nanoparticles were produced by taking as reference the methodology described by other authors, which reduces the metal precursor with ammonia borane in a methanol solution [16]. Then the samples were calcinated at 400°C during 3 hours in order to eliminate the surfactant.

Finally, in all the cases, the aerogels were milled during 60 minutes at 100 rpm with a Planetary Ball Mill PM 100 (Retsch) and the powder was treated with a flow of 2 NL/min of pure H₂ at 150°C during 30 minutes to activate the catalyst.

2.2.2 *D-glucose hydrogenation:*

The reaction was performed in batch in an experimental set-up with a commercial stainless steel high pressure reactor (Berghof BR-25) with an internal volume of 25 cm³, agitated with a magnetic stirring bar 1400 rpm and fitted up with a proportional–integral–derivative system for temperature control. The hydrogenation reaction was performed by pumping 5 mL of glucose solution (10g/L) and charging 150 mg of the hydrophilic aerogels with different loads of Pd. All the catalytic tests were performed at 120°C and 2.5 MPa of pure hydrogen during 360 min. A more detailed description of the set-up can be found elsewhere [17]. Activity of the different catalyst (A , mol_{converted}

$\text{glucose} \cdot \text{mol}_{\text{metal}}^{-1} \cdot \text{min}^{-1}$) and selectivities to the products (S, %) were calculated using Eq. (1) and Eq. (2).

$$A = \frac{n_{\text{glucose } 0} - n_{\text{glucose } f}}{n_{\text{metal}} \cdot \text{min}} \quad (1)$$

$$S (\%) = \frac{n_{\text{product}}}{n_{\text{glucose } 0} - n_{\text{glucose } f}} \quad (2)$$

2.3 Characterization:

The aerogel structure was studied by Fourier transform infrared spectra (FT-IR model TENSOR from BRUKER, Spain)

Metal loading was determined by atomic absorption (AA) using a VARIAN SPECTRA 220FS analyzer. Digestion of the samples was performed with HCl, H₂O₂ and HF using microwave at 250 °C.

The crystallinity of the impregnated Pd particles were analyzed by X-ray diffraction (Discover D8-Bruker)

A JEOL field emission microscope, model JEM-FS2200 HRP, operating at 200 kV was used for HR TEM (High Resolution Transmission Electron Microscopy) and EDX (Energy-Dispersive X-ray spectroscopy).

The textural properties of the catalysts were determined by nitrogen isothermal adsorption-desorption. A Surface Area and Porosity Analyzer (ASAP2020-Micrometrics) was used. The specific surface area was calculated by the BET (Brunauer–Emmett–Teller) method. The specific pore volume is determined by the single point adsorption method. The shown average pore diameter is based on the desorption isotherm of the Barrett-Joyes-Halenda (BJH) method.

Hydrogenation products were analyzed by liquid chromatography (HPLC). The HPLC column used was SUGAR SC-1011 from Shodex at 80 °C and a flow of 0.8 cm³·min⁻¹ using water Milli-Q as the mobile phase. A Waters IR detector 2414 was used to identify sugars, polyols and their derivatives.

3. Results

3.1 *Infrared spectra studies*

Fig. 1 shows the infrared spectra of the silica aerogel and the different synthesized catalysts. The untreated support shows some methyl groups on the surface (815, 2862, 2936 and 2974cm⁻¹); these groups are expected to correspond to residual non-hydrolyzed alkoxy groups on the surface of the silica aerogels [18]. The free metal support was also reduced under the same conditions which were used to reduce the catalysts and not important fluctuations were noticed on the spectra. By contrast a significant decrease on the methyl groups followed by an increment of the silanol peak (960 cm⁻¹) was noticed in the samples produced by WI. What is more, comparing the sample prepared at 20°C and the one at 50°C, the hydroxylation seems to be related with the temperature of the impregnation. A similar but slighter effect is observed on the sample prepared by SCI. Although the temperature of SCI is 60°C, the reduction in the methyl groups and the increment at 960cm⁻¹ is less pronounced in supercritical CO₂ than in acetone. A different phenomena is observed in the catalyst made by direct synthesis which has completely lost these methyl groups but does not show the higher intensity on the silanol region. This could be explained by the temperatures reached during the calcination of the PVP which allows the loose of the methyl groups but also the initialization of the dihydroxylation [19].

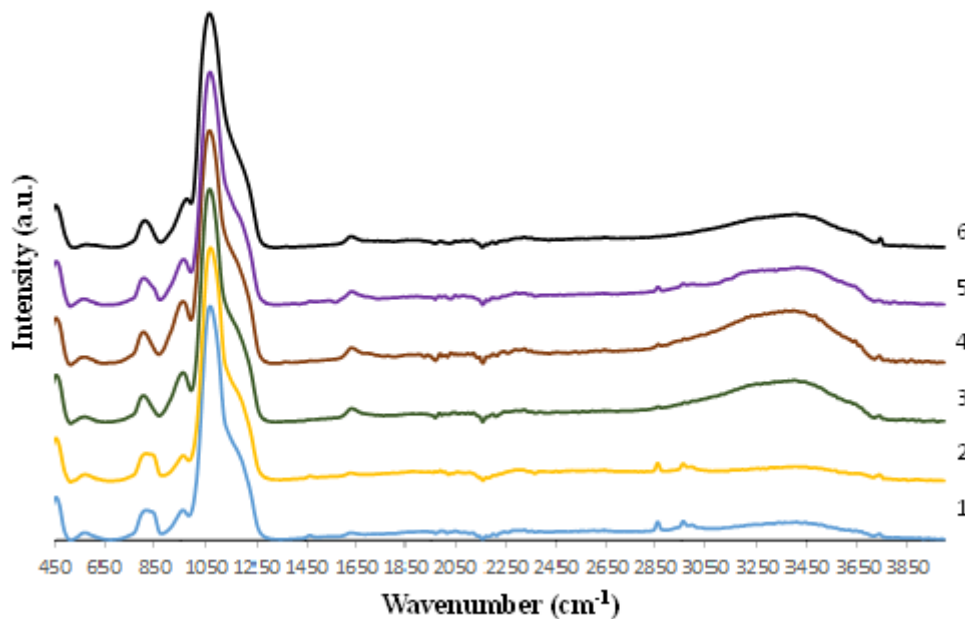


Fig. 1. Infrared spectra of the raw aerogel (1), reduced aerogel (2), reduced WI with acetone at 20°C (3), reduced WI with acetone at 50°C(4), reduced SCI (5) and reduced DS (6).

Concerning the OH stretching region, three different bands can be distinguished. The one at 3735cm^{-1} corresponds to the free silanol groups on the silica surface. The broad band at $\sim 3502\text{cm}^{-1}$ belongs to the stretching vibrations of the hydroxyl groups of water physically adsorbed on SiO_2 surface and the surface silanol groups entering into a hydrogen bond. The band at $\sim 3660\text{cm}^{-1}$ can be assigned to the hydroxyls that have formed weak hydrogen bonds [20]. The different catalysts show different intensities in these peaks, which is translated into different chemical properties of the surfaces of the materials.

3.2 Nitrogen physisorption studies

The N_2 -adsorption experiment with the raw aerogel and the activated catalyst led to the isotherms illustrated in Fig. 2. The isotherms belongs to “type IV” which is typical for mesoporous materials. The hysteresis loop is wide, and the desorption curve is more precipitous than the adsorption curve. This situation is classified as H2 type loops and usually occurs when the distributions of pore size radius are wide [21]. Like the raw

aerogel, all the catalyst present a unimodal pore size distribution except the DS one, whose distribution is bimodal.

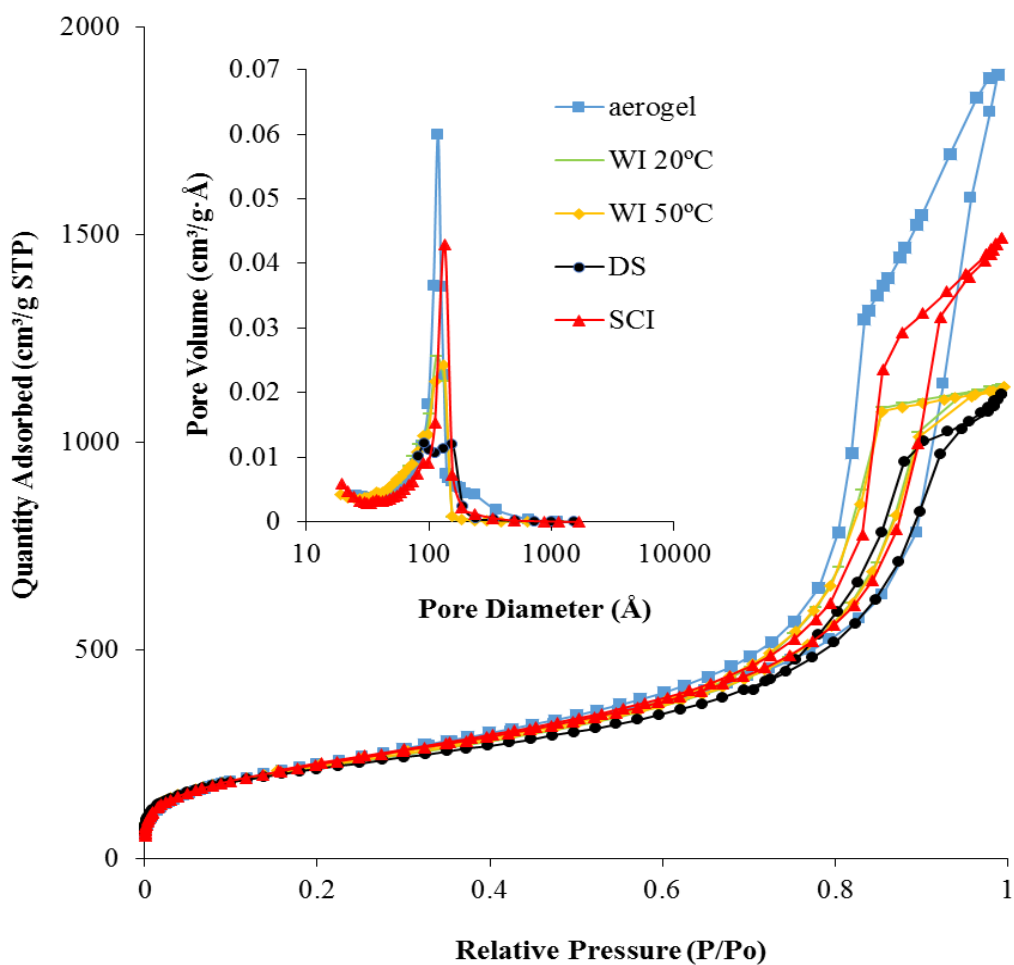


Fig. 2. Nitrogen adsorption isotherms and pore size distribution of the raw aerogel, the WI with acetone at 20°C, the WI with acetone at 50°C, the SCI and the DS

Table 1 BET surface area, pore volume and pore diameter of raw aerogel and activated catalysts

	BET Surface Area (m ² /g)	Pore Volume (cm ³ /g)	Pore diameter (\emptyset) (nm)
raw			
aerogel	845	2.91	11.66
WI 20°C	788	1.76	10.37
WI 50°C	799	1.71	8.86
SCI	825	2.31	11.13
DS	766	1.72	13.67

As shown in Table 1 the impregnated sample which keeps its final properties closer to the ones of the raw aerogel is the one prepared by SCI. Apparently this technique has allowed to block less of the pores than the WI technique because the size of the biggest particles of metal produced by SCI is smaller than the biggest particles produced by WI. Concerning this WI catalyst, the possibility of increasing the Pd loading by increasing the temperature at which the solvent is saturated with the Pd precursor does not seem to increase the number of obstructions because there is not an important effect on the textural properties. With respect to the catalyst prepared with suspended Pd nanoparticles during the sol-gel process, the drop in surface and pore volume is bigger than in the other samples and its pore diameter is the biggest. As said above, this sample is the only one with a bimodal pore size distribution. But in this case, the changes on the properties could be attributed to the thermal treatment of the sample during the calcination in order to remove the surfactant which requires temperatures of 400°C [22].

3.3 Powder X-ray diffraction studies

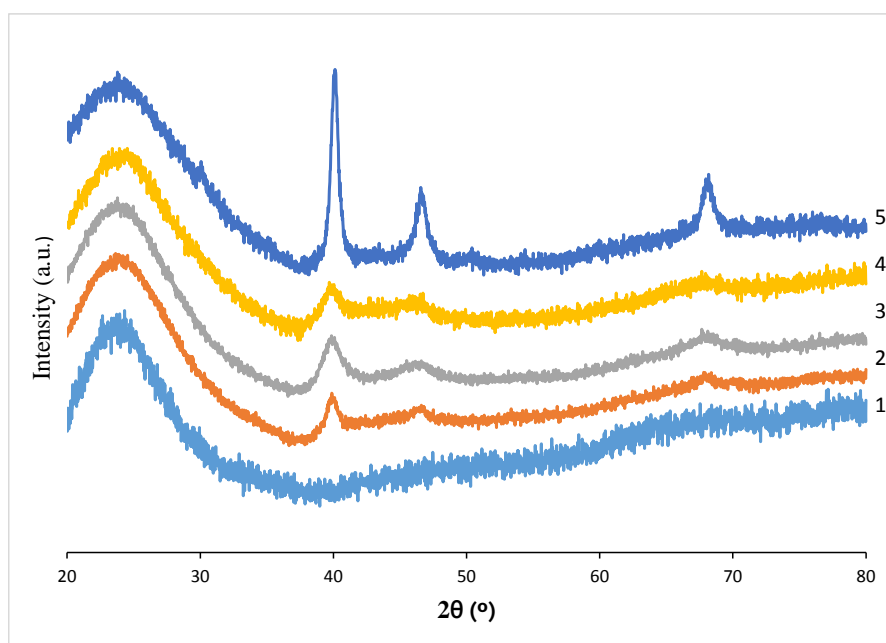


Fig. 3. X-ray diffraction patterns of silica aerogel (1) and palladium containing aerogels; WI with acetone at 20 (2) and 55°C (3), SCI (4) and DS (5) samples.

X-ray diffraction patterns for bare silica aerogel and Pd-based catalysts are shown in Fig. 3. Three characteristic diffraction peaks were detected at $2\theta=40^\circ$, 46° and 68° (JCPDS 46-1043) corresponding to the presence of (111), (200) and (220) planes [23]. This information suggested the presence of Face-Centered Cubic (FCC) Pd⁰ nanoparticles [24]. The broader base of the peaks in the cases of the WI and SCI indicate a better distribution of the metal inside the matrix[25]. No PdO peaks were observed which means that the samples were completely reduced under pure H₂. By applying the Scherrer equation to the samples prepared by WI with acetone at 20 and 50°C, SCI sample and the ones prepared by DS, the calculated crystal size are 4.4nm, 3.72 nm, 5.01 nm and 7.14 nm respectively.

3.4 *Transmission electron microscopy studies*

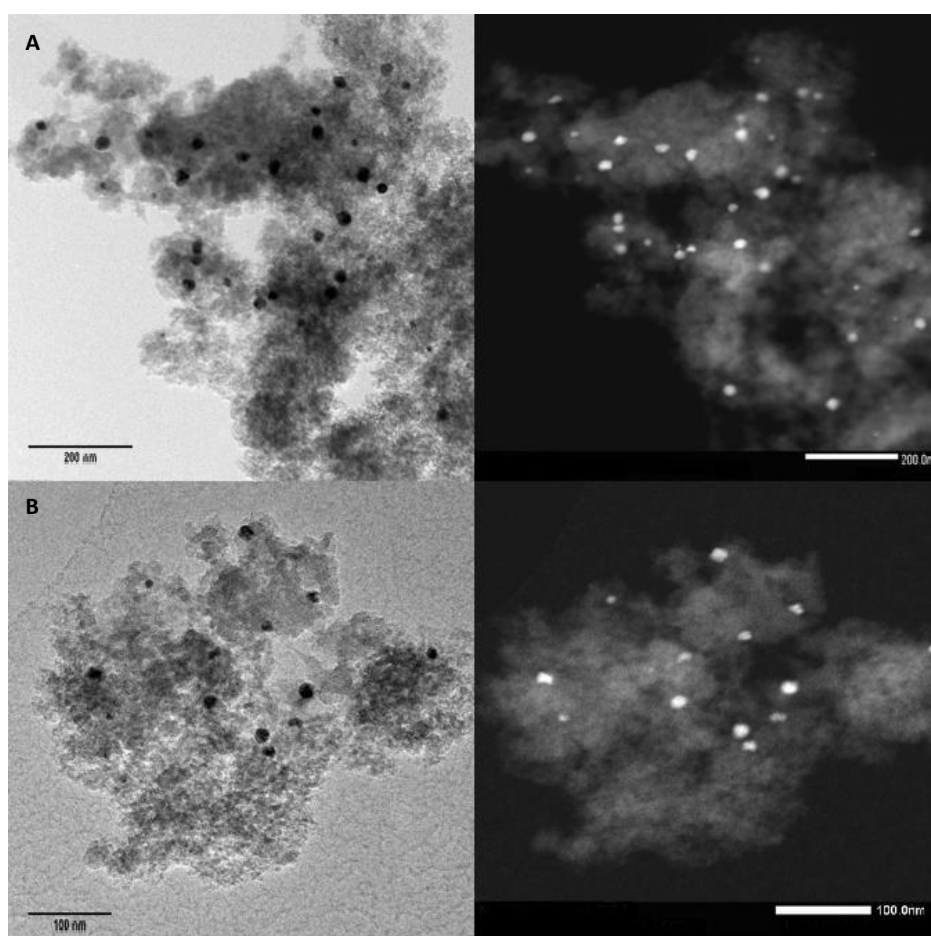


Fig. 4. HR TEM and dark field images of catalyst prepared by WI (A) and SCI (B)

Fig. 4 shows the HR TEM and dark field of the catalyst prepared by WI and SCI. Both of them present a homogeneous and well distributed particles, which is in good relation with the small and wide peaks in the X-ray spectra. Nevertheless an important variation on the size of the particles is seen; in the case of the WI, the size varies from 4 to 30nm and in the case of the SCI, from 3 to 20 nm. This variation in the size of the biggest particles could be important; it is similar to the expected pore size of the matrix, which indicates that particles with sizes in this range probably are blocking some of the pores of the aerogel scaffold.

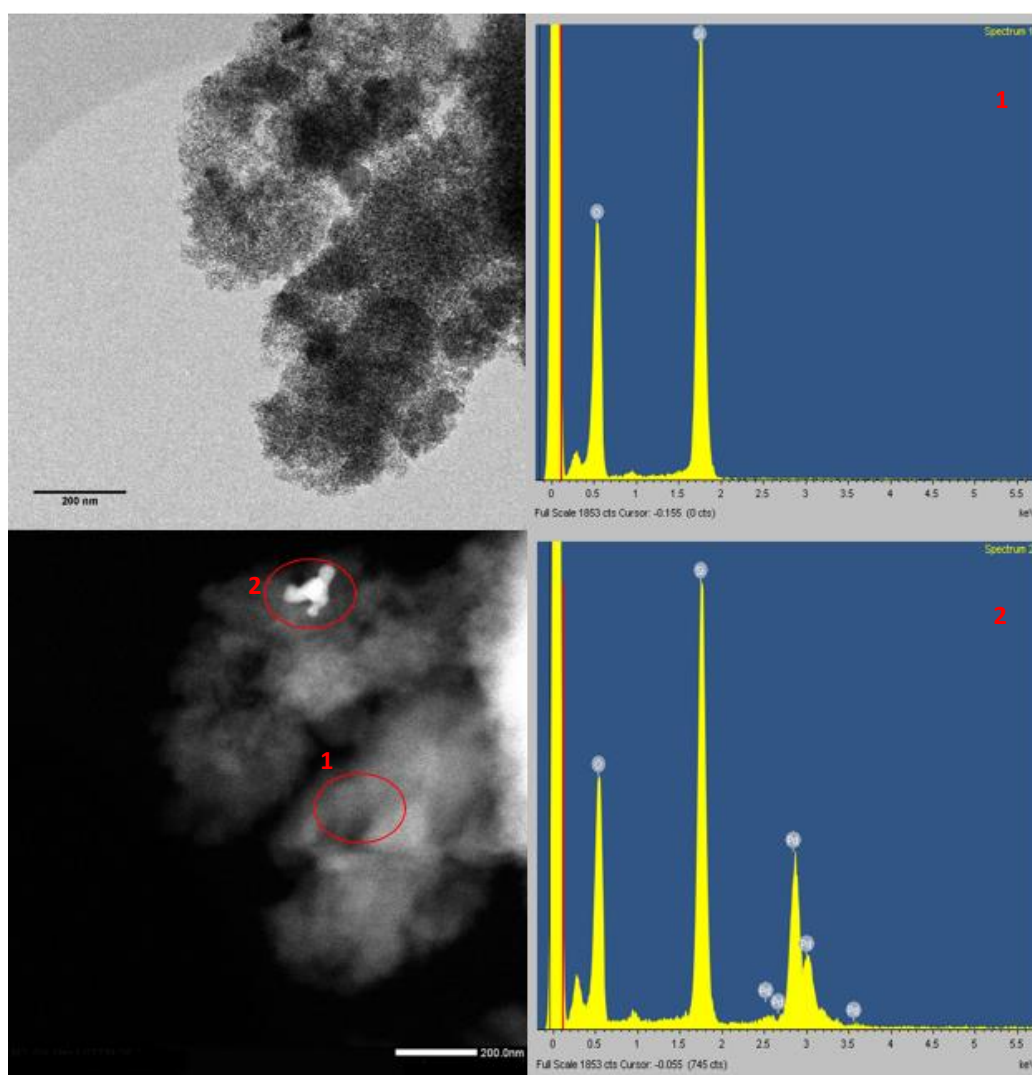


Fig. 5.HR TEM, dark field images and EDX of direct synthesis catalyst.

By contrast the images showed on Fig. 5 demonstrate the agglomeration of the metallic particles in the catalyst prepared by the direct synthesis technique. This bad distribution is also checked by comparing region 1 and 2 in the dark field. Their corresponding EDX show the presence of palladium just in region 1, without presence of palladium in the rest of the scaffold. The agglomerates present a size above 100nm. This result is in good agreement with the highest reduction on the pore volume observed in the BET analysis. This result could be due to the incorrect suspension of the Pd-PVP nanoparticles in the solvent during the sol-gel reaction. Indeed, a correct dispersion of the particles in the gel during ageing is difficult due to the high viscosity of this medium. The use of ultrasounds could be useful to overcome this defect. Another reason could be the formation of PdO during the calcination of PVP promotes the sintering due to the weaker interactions of the metallic particles with the support.

3.5 Atomic absorption studies

As can be seen in Table 2, the catalyst with less metal content was the one impregnated with methanol (0.13%). By contrast, the ones impregnated with acetone present higher concentrations from 0.54 to 1.03%. On the one hand, this gradient was achievable by increments of the impregnation solution temperature and concentration. On the other hand the low ebullition temperature of the acetone limits the maximum operating temperature, and therefore the maximum concentration of Pd(acac)₂ in the solution. It can be concluded that two effects govern the final metal content: the solubility of the precursor and the interactions between the silanol groups on the surface and the solvent. Further studies could also be done in order to check the SCI results when using other pressure and temperature conditions, resulting in other solubilities. Finally the amount of Pd on the sample prepared with suspended Pd PVP particles can be controlled by

adding more or less metal in the suspension used for the synthesis of the gels. The amount of metal added to the suspension and the final one is in good agreement.

Table 2 Metallic content on the activated catalysts

		WI			SCI	DS
P (MPa)					25	
solvent	MeOH		Acetone		Supercritical CO ₂	
T (°C)	20	20	40	50	60	
Pd wt %	0.13	0.54	0.65	1.03	0.84	1.61
Particle size (nm)				4-30	3-20	> 100

3.6 Catalytic activity studies

The results of the hydrogenations of D-glucose are summarized in Table 3 in terms of activity and selectivity. On the one hand, the materials have shown different catalytic behaviors depending on the preparation method. The catalysts prepared by WI method (WI 20°C and WI 50°C) showed the highest activity during the hydrogenation experiments and the material synthesized by DS presented the lowest one. This fact can be attributed to the different crystallite size calculated from XRD patterns and Scherrer equation, where WI 20°C and WI 50°C obtained crystallite sizes around 4 nm while DS achieved 7 nm. In addition the crystals are not just the biggest but also forms agglomerates as shown in HR TEM images (Fig. 5). Small differences in terms of activity were observed comparing both WI 20°C and WI 50°C. The higher concentration of the metal in the matrix has not been turned into a higher activity. This could be explained by the size of the particles in the matrix, which is probably bigger in the case of the catalyst with more metal content, reducing the exposed active surface of the metal. Another point to contrast is that the textural properties of the SCI sample are the best, but its activity is lower than those obtained by WI. Therefore, other factors should

be taken into account. First of all, the different concentration and nature of the hydroxyl groups on the surface seem to be playing a role. Secondly, the formation of different types of carbide on the surface due to the direct reduction under hydrogen atmosphere [26] cannot be ignored.

On the other hand, selectivity to sorbitol results presented in Table 3 demonstrated the influence of the preparation method and metal loading in the composition of the final product. Comparing both selectivities to sorbitol for WI 20°C and WI 50°C, it was observed that an increase in Pd loading from 0.54 to 1.03 % enhanced selectivity to sorbitol from 54 to 76 %. Low amounts of fructose were detected suggesting retro aldol condensation reaction to produce glyceraldehyde that is subsequently hydrogenated into glycerol which is the main byproduct in both cases. In addition, glycerol was the main compound in the liquid product when hydrogenation of D-glucose was carried out over the catalyst prepared by SCI achieving a selectivity to glycerol around 89 %. In the case of SCI sorbitol was not detected in the final product. As it was explained above, hydroxyl groups and carbide on the surface of the support could decrease the activity of the catalyst and favor glycerol production. Finally, D-glucose is hydrogenated with a selectivity around 47 % to sorbitol over the catalyst prepared by DS and no other products could be identified by HPLC in this case.

Table 3 Catalytic activity, (moles of converted glucose per moles of metal and per minute) and selectivity to sorbitol of the synthesized catalysts at 120 °C, 2.5 MPa H₂ and 360 min

	WI 20°C	WI 50°C	SCI	DS
Activity	$1.42 \cdot 10^{-2}$	$1.07 \cdot 10^{-2}$	$4.45 \cdot 10^{-3}$	$2.27 \cdot 10^{-3}$
S _{SORBITOL} (%)	54.23	75.85	0	47.26
S _{GLYCEROL} (%)	34.71	22.43	88.45	0

4. CONCLUSIONS

Three different routes have been used to impregnate silica aerogels with Pd. The load of the metal could be tuned by controlling the concentration of Pd in the different impregnation media but at the same time the achievable concentration is limited by the solubility of the precursor. Well distributed particles were obtained with WI and SCI but agglomeration was observed on the DS catalyst. The test of the catalysts in the hydrogenation of D-glucose have proved that the influence of the concentration of metal and the size of the metallic particles are important. In addition, the chemistry of the support, which is modified depending on the way in which the support is impregnated, and the presence of carbides, seem to play an important role on activity and selectivity.

Acknowledgments

This research has been financed by the Spanish Ministry of Economy and Competitiveness through project ENE2014-53459-R. Á. Martín thanks the Spanish Ministry of Economy and Competitiveness for a Ramón y Cajal research fellowship. L.M. Sanz-Moral thanks the Spanish Ministry of Economy and Competitiveness for a FPI predoctoral grant. M. Rueda thanks the University of Valladolid for a FPI predoctoral grant. A. Navarrete thanks the kind support of the FP7 Shyman European project (Project reference: 280983). A. Romero thanks to the program of predoctoral scholarships from Junta of Castilla y Leon for his grant (E-47-2015-0062773).

References

- [1] Rao AV, Pajonk GM, Parvathy NN. Influence of Molar Ratios of Precursor, Catalyst, Solvent and Water on Monolithicity and Physical Properties of TMOS Silica Aerogels. *J. Sol-Gel Sci. Technol.* 1994;3:205-217.
- [2] Venkateswara Rao A, Kulkarni MM, Amalnerkar DP, Seth T. Surface chemical modification of silica aerogels using various alkyl-alkoxy/chloro silanes. *Appl. Surf. Sci.* 2003;206(1-4):262-270.
- [3] Maleki H, Durães L, Portugal A. An overview on silica aerogels synthesis and different mechanical reinforcing strategies. *J. Non-Cryst. Solids* 2014;385:55-74.
- [4] Heinrichs B, Noville F, Pirard JP. Pd/SiO₂-Cogelled Aerogel Catalysts and Impregnated Aerogel and Xerogel Catalysts: Synthesis and Characterization. *J. Catal.* 1997;170:366-376.
- [5] Martínez S, Vallribera A, Cotet CL, Popovici M, Martín L, Roig A, Moreno-Mañas M, Molins E. Nanosized metallic particles embedded in silica and carbon aerogels as catalysts in the Mizoroki–Heck coupling reaction. *New J. Chem.* 2005;29:1342-1345.
- [6] Anderson K, Cortiñas Fernández S, Hardacre K, Marr PC. Preparation of nanoparticulate metal catalysts in porous supports using an ionic liquid route; hydrogenation and C–C coupling. *Inorg. Chem. Commun.* 2004;7:73–76.
- [7] Morley KS, Licence P, Patricia CM, Hyde JR, Brown PD, Mokaya R, Xia Y, Howdle SM. Supercritical fluids: A route to palladium-aerogel nanocomposites. *J. Mater. Chem.* 2004;14:1212-1217.
- [8] Yoda S, Hasegawa A, Suda H, Uchimaru Y, Haraya K, Tsuji T, Otake K. Preparation of a Platinum and Palladium/Polyimide Nanocomposite Film as a Precursor of Metal-Doped Carbon Molecular Sieve Membrane via Supercritical Impregnation. *Chem. Mater.* 2004;16:2363-2368.

- [9] Mishra DK, Dabbawala AA, Park JJ, Jhung JP, Sung SH, Hwang JS. Selective hydrogenation of d-glucose to d-sorbitol over HY zeolite supported ruthenium nanoparticles catalysts. *Catal. Today*. 2014;232:99-107.
- [10] Heinen AW, Peters JA, van Bekkum H. Hydrogenation of fructose on Ru/C catalysts. *Carbohydr. Res.* 2000;328:449-457.
- [11] Cantero DA, Sánchez Tapia Á, Bermejo MD, Cocero MJ. Pressure and temperature effect on cellulose hydrolysis in pressurized water. *Chem. Eng. J.* 2015; 276:145-154.
- [12] Lazaridis A, Karakoulia S, Delimitis A, Coman SM, Parvulescu VI, Triantafyllidis KS. d-glucose hydrogenation/hydrogenolysis reactions on noble metal (Ru, Pt)/activated carbon supported catalysts. *Catal. Today*. 2015;257:281-290.
- [13] Bizhanov FB, Sokol'sskii DV, Popov NI, Malkina NYa, Khisametdinov AM. *kinetica I kataliz*, 1967; 8: 620.
- [14] Novak Z, Knez Z. Diffusion of methanol-liquid CO₂ and methanol-supercritical CO₂ in silica aerogels *J. Non-Cryst. Solids*. 1997;221:163-169.
- [15] Sanz-Moral LM, Rueda M, Mato R, Martín Á. View cell investigation of silica aerogels during supercritical drying: Analysis of size variation and mass transfer mechanisms . *J. Supercrit. Fluids* 2014;92:24-30.
- [16] Erdogan H, Metin Ö, Özkar . In situ-generated PVP-stabilized palladium(0) nanocluster catalyst in hydrogen generation from the methanolysis of ammonia-borane *Phys. Chem. Chem. Phys.* 2009;11:10519-10525.
- [17] Romero A, Alonso E, Sastre A, Nieto-Márquez A. Conversion of biomass into sorbitol: Cellulose hydrolysis on MCM-48 and D-glucose hydrogenation on Ru/MCM-48. *Microporous Mesoporous Mater.* 2016;224:1-8.

- [18] Sanz-Moral LM, Rueda M, Nieto A, Novak Z, Knez Z, Martín Á. Gradual hydrophobic surface functionalization of dry silica aerogels by reaction with silane precursors dissolved in supercritical CO₂. *J. of Supercritical Fluids*.2013;84:74–79.
- [19] Cui S, Liu Y, Fan M, Cooper AT, Lin B, Liu X, Han G, Shen X. Temperature dependent microstructure of MTES modified hydrophobic silica aerogel. *Mater. Lett.* 2011;65:606–609.
- [20] Yi-hua Xie, Bing Li, Wei-Zheng Weng, Yan-Ping Zheng, Kong-Tao Zhu, Nuo-Wei Zhang, Chuan-Jing Huang, Hui-Lin Wan. Mechanistic aspects of formation of sintering-resistant palladiumnanoparticles over SiO₂prepared using Pd(acac)₂as precursor *Appl. Catal.* 2015;504:179–186.
- [21] Wang W, Liu P, Zhang M, Hu J, Xing F. The Pore Structure of Phosphoaluminate Cement. *Open Journal of Composite Materials.* 2012;2:104-112.
- [22] Wagh PB, Pajonk GM, Haranath D, Rao AV. Influence of temperature on the physical properties of citric acid catalyze TEOS silica aerogels. *Mater. Chem. Phys.* 1997;50:76–81.
- [23] Habibi B, Mohammadyari S. Palladium nanoparticles/nanostructured carbon black composite on carbon–ceramic electrode as an electrocatalyst for formic acid fuel cells. *J. Taiwan Inst. Chem. Eng.* 2016;58:245-251
- [24] Teranishi T, Miyake M. Size Control of Palladium Nanoparticles and Their Crystal Structures. *Chem. Mater.* 1998;10:594-600.
- [25] Kibombo HS, Balasanthiran V, Wu CM, Peng R, Koodali RT. Exploration of room temperature synthesis of palladium containing cubic MCM-48 mesoporous materials. *Microporous Mesoporous Mater.* 2014;198:1-8.
- [26] Daniell W, Landes H, Fouad NE, Knözinger H. Influence of pretreatment atmosphere on the nature of silica-supported Pd generated via decomposition of

Pd(acac)₂: an FTIR spectroscopic study of adsorbed CO. *J. Mol. Catal. A: Chem.*
2002;178: 211–218